ACS OMEGA

http://pubs.acs.org/journal/acsodf

Article

Cross-Talk of Protein Expression and Lysine Acetylation in Response to TMV Infection in *Nicotiana benthamiana*

Liyun Song,[#] Huaixu Zhan,[#] Yujie Wang, Zhonglong Lin, Bin Li, Lili Shen, Yubing Jiao, Ying Li, Fenglong Wang,* and Jinguang Yang*

Cite This: *ACS Omega* 2022, 7, 32496−32511

Read Online

ACCESS | Metrics & More | Article Recommendations | Supporting Information

ABSTRACT: Lysine acetylation (K^{ac}), a reversible PTM, plays an essential role in various biological processes, including those involving metabolic pathways, pathogen resistance, and transcription, in both prokaryotes and eukaryotes. TMV, the major factor that causes the poor quality of Solanaceae crops worldwide, directly alters many metabolic processes in tobacco. However, the extent and function of K^{ac} during TMV infection have not been determined. The validation test to detect K^{ac} level and viral expression after TMV infection and Nicotinamide (NAM) treatment clarified that acetylation was involved in TMV infection. Furthermore, we comprehensively analyzed the changes in the proteome and acetylome of TMV-infected tobacco (*Nicotiana benthamiana*) seedlings via LC−MS/MS in conjunction with highly sensitive immune-affinity purification. In total, 2082 lysine-acetylated sites on 1319 proteins differentially expressed in response to TMV infection were identified. Extensive bioinformatic studies disclosed changes in acetylation of proteins engaged in cellular metabolism and biological processes. The vital influence of K^{ac} in fatty acid degradation and alpha-linolenic acid metabolism was also revealed in TMV-infected seedlings. This study first revealed K^{ac} information in *N. benthamiana* under TMV infection and expanded upon the existing landscape of acetylation in pathogen infection.

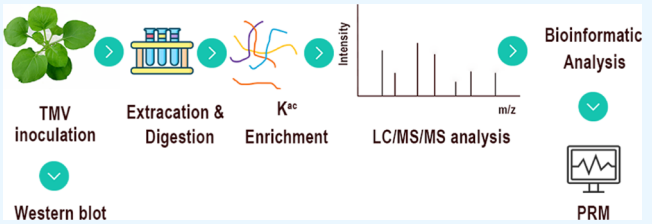

INTRODUCTION

Post-translational modifications (PTMs) play crucial roles during the growth of eukaryotes and prokaryotes.[1] More than 450 PTMs[2] have been reported to be associated with many biological processes, such as transcriptional regulation, protein degradation, metabolism, stress responses, and plant disease resistance.[3−7] As a highly conserved PTM, lysine acetylation (K^{ac}) shows great potential for functional regulation.[8,9] Two forms of K^{ac} have been identified: N alpha acetylation and N ε acetylation. The former occurs on the alpha-amino group at the N-terminus of the protein, the modification of which is usually irreversible and common among eukaryotes. The latter occurs on the ε-amino group on the side chain of lysine, which is dynamic and convertible in both eukaryotes and prokaryotes.[10,11] K^{ac} is catalyzed by lysine acetyltransferases (KATs) and reversed by lysine deacetylases (KDACs).[12]

According to extensive studies on the influence of acetylation on gene transcription,[13] this modification regulates numerous biological processes, such as those involving metabolic pathways,[14−16] pathogen responses,[17] stress responses,[18−20] protein interactions,[21] enzymatic activity,[22,23] and protein stability.[24] Due to the rapid development of liquid chromatography−mass spectrometry (LC−MS/MS) and affinity purification, numerous analyses of the lysine acetylome have been reported.[1,11,12,25] Compared with the massive number of K^{ac} studies in microbes and mammals, the number of acetylome studies in plants is lower.[26] Especially in the field of plant pathology, few studies on the acetylome of plant resistance[27−30] and in response to pathogenic microbes[31−35] and biocontrol microbes[36−39] have been reported. How pathogens adjust host plants to respond to infection is a major concern in biology. It has been shown that the acetylation level of plant protein changes significantly after infection by the pathogen. For example, the acetylation level of *Paulownia tomentosa* changes significantly in response to phytoplasma infection.[40] *Citrus sinensis* histone modification genes show obvious alterations in their expression levels during the *Penicillium digitatum* infection.[41] Fungal pathogens promote the susceptibility in soybean and maize through altering protein acetylation.[29] The regulation of the acetylation level or disease resistance in plants after pathogen infection is also different. In soybean, the cytoplasmic effector PsAvh23 generated by *Phytophthora sojae* works as a modulator of histone acetyltransferase (HAT), which suppresses H3K9 acetylation and enhances plant susceptibility.[29] Similarly,

Received: June 26, 2022
Accepted: August 23, 2022
Published: September 1, 2022

HC-toxin (HCT), a histone deacetylase inhibitor (HDACI), produced by the fungal pathogen *Cochliobolus carbonum* race 1, leads to an ineffective defense reaction in maize via changing protein acetylation.[7] Additionally, some studies find a relationship between gene expression of acetylation enzymes and pathogen infection. For example, Ding et al.[42] report that the expression level of plant-specific HD2 subfamily of histone deacetylases (HDACs) in rice alters as a result of infection by the fungal pathogen *Magnaporthe oryzae*. Xing et al.[43] demonstrate that the expression of four *SiHATs* (*HAT* genes) is changed after infection with *Sclerospora graminicola*. These studies demonstrate that acetylation is involved in the process of pathogen infection and plant reaction. However, the characteristics of acetylation in host plants after viral infections have rarely been reported. Therefore, research on the acetylome of host plants during disease resistance may be important in illuminating the functional characteristics of acetylated proteins for phytopathology.

In this work, we used tobacco (*Nicotiana benthamiana*) as a material, which is a model plant species widely used in molecular biological research. The validation test revealed that TMV infection resulted in altered acetylation levels and that K^{ac} may contribute to viral infection. Large-scale analysis of the acetylome of *N. benthamiana* seedlings was performed via high-resolution liquid chromatography−tandem mass spectrometry (LC−MS/MS) combined with anti-acetyl lysine antibody-based immune-affinity enrichment and intensive bioinformatic tools. Altogether, 2082 acetylation sites distributed across 1319 proteins took part in multiple cellular compartments, including peroxisomes, microbodies, the chloroplast envelope, and the plastid envelope; these proteins mostly participated in the fatty acid metabolic process and the alpha-linolenic acid metabolic process. Therefore, the elucidation of acetylation levels after TMV infection in *N. benthamiana* could provide an abundance of data for recognizing the prospective role of this modification in virus resistance. The results not only greatly broaden the existing field of K^{ac} research but also clarify the importance of acetylome in plant pathology.

EXPERIMENTAL SECTION

Sample Preparation. Tobacco (*N. benthamiana*) plants were cultivated in a greenhouse with a 16/8 h (light/dark) photoperiod at 25 °C. After 4 weeks of growth, the leaves of three replicate tobacco seedlings were collected for subsequent experiments. We used a previous method[44] to prepare TMV solution. Tobacco leaves were gathered at 2, 4, 6, and 8 days post-inoculation (dpi). We used PBS-treated tobacco seedlings as controls. Each biological sample was prepared and assessed in triplicate.

Nicotinamide (NAM) Treatment. After the *N. benthamiana* seedlings had grown for 4 weeks, consistent growth was observed, and NAM and the control reagent dimethyl sulfoxide (DMSO) were diluted to the same concentrations. The abaxial side of the leaves was infiltrated with the solutions with a needleless syringe, and the same position of the leaves for each treatment was used. Three biological replicates were included for each treatment. Inoculation with TMV solution was performed 2 h later, and samples were taken 24 and 48 h after inoculation and then stored at −80 °C for later use.

Western Blotting Analysis. Proteins were isolated from samples that had been inoculated with PBS and TMV solutions at different time points. We used a commercial antibody against acetylation on Western blot analysis as previously reported.[26,45] The proteins were isolated by sodium dodecyl sulfate−polyacrylamide gel electrophoresis (SDS−PAGE) and then transferred to a polyvinylidene fluoride (PVDF) membrane (Immobilon-P, Merck Millipore, United States). The TMV coat protein (cp) antibody (Agdia, Elkhart, United States), anti-rabbit secondary antibody (CWBIO, Beijing, China), and beta-actin (CWBIO, Beijing, China) antibody were used for the analysis. Anti-acetyl-lysine was used as a primary antibody (Micron Bio, Hangzhou, China) and the anti-mouse secondary antibody conjugated to HRP (CWBIO, Beijing, China). The Western blot results were analyzed using ImageJ (v.1.52a, NIH, Bethesda, USA).

Protein Extraction, Trypsin Digestion, and TMT Labeling. Tobacco samples were ground and resuspended in lysis buffer comprising 10 mM dithiothreitol (DTT), 1% Triton X-100, 8 M urea, and 1% protease inhibitor cocktail. Next, the extracts were sonicated three times on ice, and the debris was centrifuged at 20,000*g* at 4 °C for 10 min. Finally, the proteins were precipitated with cold 20% trifluoroacetic acid (TCA) for 2 h at −20 °C. The supernatant was removed after centrifugation at 4 °C and 12,000*g* for 10 min, and the remaining protein precipitate was subsequently rinsed with cold acetone three times. The protein content in the supernatant was measured using a 2-D Quant Kit (GE Healthcare, Pittsburgh, USA) following the manufacturer's protocol.

The protein solution was reduced using 5 mM DTT for 45 min at 30 °C and then alkylated with 30 mM iodoacetamide (IAA) for 1 h in darkness. The sample was then diluted by the addition of 0.1 M triethylammonium bicarbonate (TEAB) such that the urea concentration was adjusted to less than 2 M. Finally, trypsin (1/25 protein mass) was used for primary digestion for 12 h at 37 °C; the reaction was ended with 1% trifluoroacetic acid (TFA).

Then, the samples were desalted with a Strata X C18 SPE column (Phenomenex, Torrance, USA) and dried in vacuum. The peptides were reconstituted in 0.5 M TEAB following the producer's protocol for a six-plex TMT kit (Thermo, Waltham, USA). One unit of TMT reagent (the amount of reagent needed to label 5 mg of protein) was thawed and reconstituted in 420 μL of acetonitrile (ACN). The samples and four TMT reagents (126, 127, 128, 129, 130, and 131) were mixed separately, incubated for 2 h, pooled together, desalted, and dried by vacuum centrifugation. Finally, the labeled samples were resuspended in water and mixed for acetylation enrichment and proteomic analysis.

High-Performance Liquid Chromatography (HPLC) Fractionation and Affinity Enrichment. The samples were fractionated by high-pH reversed-phase HPLC using an XBridge Shield C18 RP column (Waters, Milford, USA) and an LC20AD HPLC system (Shimadzu, Kyoto, Japan). Briefly, the peptides were first separated through a gradient of 5−80% ACN in 5 mM ammonium hydroxide (pH 10) for more than 98 min into 98 fractions. The peptides were combined into 7 fractions for acetylation enrichment and 15 fractions for proteomic analysis and then dried by vacuum centrifugation for affinity enrichment.

To enrich K^{ac} peptides, tryptic peptides were dissolved in NETN buffer (0.5% NP-40, 50 mM Tris-HCl, 100 mM NaCl, 1 mM EDTA, pH 8.0) and incubated with prewashed antibody beads (Micrometer Biotech, Hangzhou, China) at 4 °C overnight under slow shaking. The beads were subsequently washed four times by NETN buffer and twice by ddH_2O. We

https://doi.org/10.1021/acsomega.2c03917
ACS Omega 2022, 7, 32496−32511

used 0.1% TFA to elute the bound peptides from the beads. Then, the eluted fractions were combined and dried in vacuum. The resulting peptides were cleaned with C18 ZipTips (Millipore, Billerica, USA), after which they were subjected to LC−MS/MS analysis.

LC−MS/MS Analysis. The peptides were dissolved in 0.1% formic acid (solvent A) and loaded onto a reversed-phase precolumn (Acclaim PepMap 100 C18 trap column, Thermo, Waltham, USA) connected to a reversed-phase analytical column (Acclaim PepMap RSLC C18, Thermo, Waltham, USA). The peptides were separated with a linear gradient of 0.1% formic acid (FA) and 80% ACN (solvent B) at a flow rate of 300 nL/min on an Easy-nLC 1000 ultra-high-performance liquid chromatography (UPLC) system (Thermo, Waltham, USA). The gradient was as follows: 0−6 min, 2−10% solvent B; 6−51 min, 10−20% solvent B; 51−53 min, 20−80% solvent B; 53−57 min, 80% solvent B; 57−58 min, 20−80% solvent B; and 58−65 min, solvent B at 2%. The peptides were analyzed via MS/MS with a system coupled to a Q Exactive HFX (Thermo, Waltham, USA) coupled to a UPLC system. MS spectra were acquired with the Orbitrap analyzer with a resolution set at 70,000, and the m/z scan range was set at 350−1500. The electrospray voltage was 2.2 kV. A data-dependent procedure that alternated between one MS scan, followed by 20 (proteome) or 15 (acetylome) MS/MS scans, was executed for the top N precursor ions above a threshold of 5×10^4 or 2.5×10^3, with a 15 s dynamic exclusion. An NCE setting of 28% was used for MS/MS analysis. Ion fragments were checked in Orbitrap at a resolution of 17,500. Automatic gain control (AGC) was applicated to prevent overfilling of Orbitrap. 3×10^6 ions accumulated to generate the MS spectra, and 5×10^4 ions accumulated to generate the MS/MS spectra. The maximum injection time was 250 ms for the MS scan and 200 ms for the MS/MS scan.

Database Analysis. *Proteome Database Search.* The resulting raw data were analyzed with the MaxQuant search engine (v.1.5.2.8). The MS/MS data were queried against the protein database of *N. benthamiana*. The mass tolerance was set at 10 ppm for precursor ions; the mass tolerance for fragment ions was set at 0.02 Da. Trypsin was selected for enzyme specificity, and two missed cleavages were allowed. The fixed modifications were carbamidomethyl on Cys and TMT-6-plex tags on Lys and peptide N-terminal regions, respectively. Oxidation of Met and TMT-6-plex tags on Tyr was specified as a variable modification. The decoy (reverse) database was used to predict the false discovery rate (FDR). Peptide−spectrum matches (PSMs), for which the p value was <0.05 and the e-value was <0.05, were considered highly acceptable.

Acetylome Database Search. The resulting raw data were managed using the MaxQuant search engine (v.1.5.2.8). We used the reverse Decoy database to search tandem mass spectra against the same database concatenated. The maximal missed cleavage of trypsin/P was 4. For precursor ions, the mass tolerance was set at 10 ppm, and the mass tolerance for fragment ions was set at 0.02 Da. The fixed modifications were carbamidomethyl on Cys and oxidation of Met. The variable modification was acetylation of lysine. The FDR threshold values for proteins, peptides, and modification sites were set to 1%. The minimal peptide length was seven amino acids (aa), and the site localization probability was set to >0.75. TMT-6-plex was selected for quantification; the other parameters in the MaxQuant analysis were set to their default values.

Bioinformatic Analysis. Gene ontology (GO) classification information was obtained from the UniProt-GOA database (http://www.ebi.ac.uk/GOA/), which resulted in the classification of lysine-acetylated proteins into biological processes, cellular components, and molecular functions.[46] Functional domains were interpreted using the InterProScan online service tool (http://www.ebi.ac.uk/interpro/). The Kyoto Encyclopedia of Genes and Genomes (KEGG) database was applied to annotate the protein pathways with the KEGG Automatic Annotation Server (KAAS), and the results were mapped using a KEGG Mapper.[47] We used WoLF PORT software (http://wolfpsort.org/) to analyze subcellular localizations.[48] Motif-X software (http://motif-x.med.harvard.edu/) was used to analyze the sequences constituted with amino acids at specific positions of modifying 21-mers (10 aa upstream and downstream of the acetylation site). All protein sequences were used as background parameters.[49] The "heatmap.2" function in the "gplot2" R package (v.2.0.3) was used to represent the cluster memberships in a heatmap format. NetSurfP software was used to determine the secondary structures of the proteins.[50] The involved functions and pathways of the modified proteins were subjected to functional enrichment analyses. GO functional enrichment, KEGG pathway, and protein domain analyses were conducted using the DAVID v.6.7 bioinformatic resources.[51] Two-tailed Fisher's exact test was utilized to test the enrichment of the differentially expressed proteins against all acetylated proteins. Any term with an adjusted p value of <0.05 in any cluster was considered significant. For TMT quantification, a comparison of protein expression was conducted by two-sample, two-sided t tests. The threshold values of differentially expressed modified and unmodified proteins were selected as a fold change ≥1.30 or ≤0.77 and $p < 0.05$. A protein−protein interaction (PPI) network of the determined proteins was described using STRING software (http://string-db.org/). We use Cytoscape (v.3.7.0) software (http://www.cytoscape.org/) to visualize the PPI network map.[52,53] Densely connected regions were analyzed with molecular complex detection (MCODE).[54] PAIL (v.1.0) software (http://bdmpail.biocuckoo.org/prediction.php) was used to predict the acetylation on internal lysines.

PRM Analysis. Peptide samples were prepared using the acetylomic analysis methodology described above. The equivalent digested peptide sample was initially run through a Thermo Q Exactive HFX (Thermo, Waltham, USA), which was connected to the UPLC with the identical gradient for subsequent PRM detection. According to the results of preliminary experiments, a total of eight peptides were chosen for analysis in the PRM assay. The peptide sample was injected onto a reversed-phase C18 column (75 μm × 25 cm, Thermo, Waltham, USA) and separated using an Easy-nLC 1200 UPLC system (Thermo, Waltham, USA). The UPLC gradient was 6% solvent B (0.1% formic acid in 80% ACN) for 1 min, 6−28% solvent B for 75 min, 28−60% solvent B for 3 min, 60−90% solvent B for 2 min, and 90% solvent B for 9 min, with a flow rate of 250 nL/min. A full mass spectrum was performed via the Orbitrap at a resolution of 60,000 (the maximum injection time was 20 ms; the AGC target was set at 3×10^6; and the m/z range was 350−1800), followed by 20 MS/MS scans on the Orbitrap at a resolution of 30,000 (AGC target was 5×10^4, and the maximum injection time was 200 ms) in a data-independent mode. The isolation window for MS/MS was set to 1.4 m/z, and the NCE was 25% with HCD. The raw data

https://doi.org/10.1021/acsomega.2c03917
ACS Omega 2022, 7, 32496−32511

were subsequently analyzed using Proteome Discoverer software v.2.2 (Thermo, Waltham, USA). The FDR was set to 0.01 for peptides. Three biological replicates were analyzed. Skyline (v.3.6) software was used for quantitative data processing and acetylomic analysis.

RESULTS

Validation Test of K^{ac} Levels under TMV Infection. The correlation between TMV inoculation and tobacco acetylation was examined by Western blotting. Protein samples were collected at 2, 4, 6, and 8 days post-inoculation (dpi). The expression of TMV CP showed an increasing tendency over time, with the highest expression at 8 dpi (Figure 1a). No changes were observed in the mock samples. In addition, the result showed that TMV infection could induce changes in acetylation levels; a strong immunoblot signal was observed at 8 dpi (Figure 1b). The upward trend between the TMV replication expression in *N. benthamiana* and the acetylation level was similar. Therefore, we chose the eighth day as the quantitative analysis time point for acetylation. We also analyzed the K^{ac} level of TMV-infected *N. benthamiana* treated with Nicotinamide (NAM), which is an inhibitor of SIRT family deacetylases (Figure 1c). Using the specific antibody of acetylation and TMV CP, we detected the acetylation level and TMV expression in the NAM-treated samples, respectively. The results showed that the level of acetylation in NAM-treated plants was upregulated, and the expression of TMV was also higher than that of the control group (Figure 1c). These results suggest that K^{ac} can be triggered by TMV infection and provide a hypothesis that acetylation of the host is involved in and may contribute to viral infection.

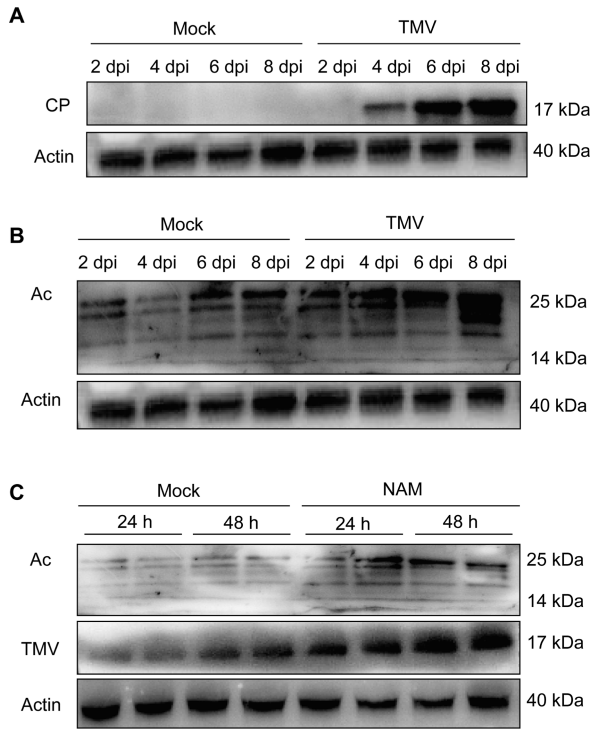

Figure 1. Validation test of K^{ac} participated in TMV infection. (a) Expression of TMV CP was detected at 2, 4, 6, and 8 dpi. *N. benthamiana* leaves inoculated with PBS were used as a mock. (b) Detection of K^{ac} in TMV-infected *N. benthamiana* leaves at a protein level. *N. benthamiana* leaves inoculated with PBS were used as a mock. (c) K^{ac} level and TMV CP expression of TMV-infected *N. benthamiana* treated with the deacetylase inhibitor NAM at 24 and 48 h. *N. benthamiana* leaves inoculated with DMSO were used as a mock.

Basic Analysis on the Quantitative Proteome. A comprehensive proteomic analysis was conducted to identify proteins whose abundance differed between the control samples and TMV-infected samples. The results reflected the high reproducibility of the MS data (Supporting Information Figure S1a). The distribution of mass error was close to zero (Supporting Information Figure S1b), which means the data were accurate for use in subsequent experiments. The length of most K^{ac} peptides ranged from 7 to 28 amino acids (Supporting Information Figure S1c). We identified 8828 acetylated proteins, of which 7218 were quantified (Supporting Information Table S1).

TMV Infection Alters Protein Expression Levels in *N. benthamiana*. To thoroughly understand the characteristics of the quantified proteins in *N. benthamiana* infected by TMV, subcellular localization, GO classification, and protein annotation information were analyzed. The proteome results indicated that TMV infection influenced the whole proteome of *N. benthamiana*. Differentially expressed proteins in different comparison groups are shown in Supporting Information Table S2. In total, 1339 proteins were associated with the inoculation of TMV. Among them, 703 proteins were upregulated, while 636 proteins were downregulated.

A GO functional classification was performed to obtain a holistic view of the proteins related to TMV (Supporting Information Figure S2a-c). The analysis of the biological process indicated that most of the differentially expressed proteins were involved with cellular processes (557; 23%), metabolic processes (479; 20%), responses to stimuli (378; 16%), and biological regulations (224; 9%). The majority of proteins in the cellular component category were related to cells, intracellular components, and protein-containing complexes. According to the molecular function classification, 53 and 30% of the differentially expressed proteins were related to catalytic activity and binding, respectively. Subcellular localization analysis (Supporting Information Figure S2d) indicated that most of these proteins were allocated in the chloroplast (38%), cytoplasm (24%), nucleus (15%), and plasma membrane (8%). The results suggested that TMV infection affects various biological processes in *N. benthamiana*.

Functional enrichment of the differentially expressed proteins was performed through GO functional enrichment, KEGG pathway, and protein domainanalyses. Biological process enrichment demonstrated that the differentially expressed proteins were mainly related to the isoprenoid metabolic process, toxin catabolic process, isoprenoid biosynthetic process, and terpenoid metabolic process (Figure 2a, blue bars). Most differentially expressed proteins in the molecular function enrichment category were related to auxin efflux transmembrane transporter activity, efflux transmembrane transporter activity, and auxin transmembrane transporter activity (Figure 2a, yellow bars). The enrichment results revealed that proteins associated with the organellar ribosome, organellar large ribosomal subunit, extracellular region, plastid large ribosomal subunit, and magnesium chelatase complex were most likely to be impacted by TMV (Figure 2a, red bars). In addition, KEGG pathway enrichment analysis revealed that a majority of differentially expressed proteins participated in alpha-linolenic acid metabolism,

https://doi.org/10.1021/acsomega.2c03917
ACS Omega 2022, 7, 32496−32511

Figure 2. Enrichment analysis of differentially expressed proteins responded to TMV infection. (a) Enrichment analysis based on GO analysis. (b) Enrichment analysis based on the KEGG pathway. (c) Enrichment analysis based on the protein domain. The numbers on the X axes represent significant values.

https://doi.org/10.1021/acsomega.2c03917
ACS Omega 2022, 7, 32496−32511

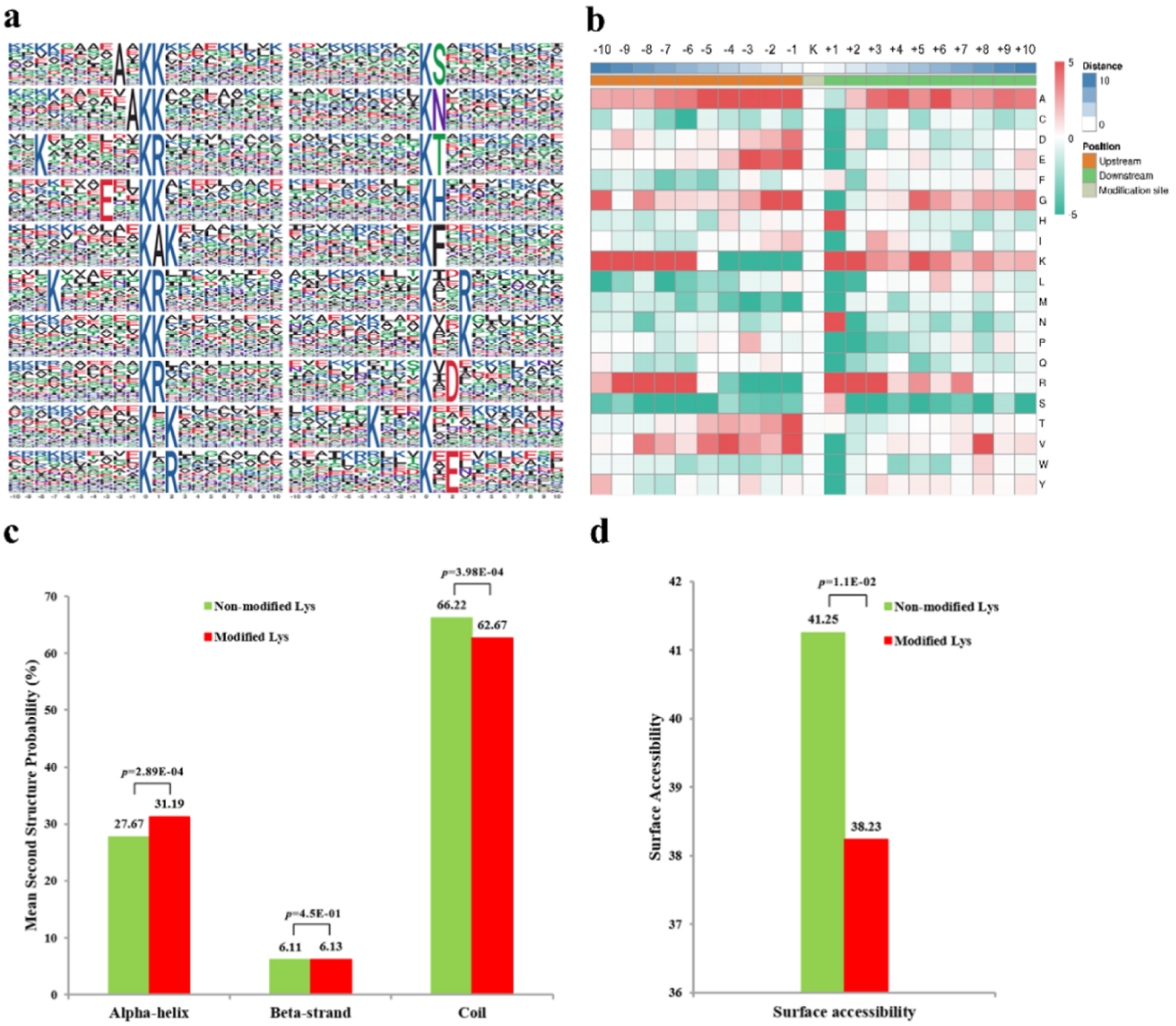

Figure 3. Bioinformation analysis of lysine-acetylated sites. (a) Acetylation motifs and conservation of acetylation sites in response to TMV. (b) Heatmap of the amino acid composition of acetylation sites. (c) Distribution of secondary structures containing lysine-acetylated sites. (d) Predicted surface accessibility of acetylated sites.

porphyrin and chlorophyll metabolism, fatty acid degradation, terpenoid backbone biosynthesis, and phenylpropanoid biosynthesis (Figure 2b). Moreover, the result of protein domain enrichment indicated that these TMV-related proteins mainly contained the following parts: "protein of unknown function, DUF642", "glutathione S-transferase, C-terminal domain", "glutathione S-transferase, N-terminal domain", and "Thaumatin family" domains (Figure 2c).

Analysis of Acetylated Proteins in Response to TMV in *N. benthamiana*. Previous studies have revealed that acetylation can affect various metabolism- and biological process-related proteins. Recent research studies have verified that K^{ac} plays a vital role in cellular metabolism and regulation in plants, animals, bacteria, and humans.[26,55,56] In this study, we used HPLC−MS/MS along with enrichment analysis to identify K^{ac} peptides in *N. benthamiana*, which is recognized as a model plant species for molecular biology research. The MS data revealed 3176 acetylation sites on 1887 proteins, of which 2082 acetylation sites on 1319 proteins were totally quantified in control plants and TMV-infected plants (Supporting Information Table S3). Acetylated proteins were expected to be upregulated if the fold change was greater than 1.3 compared with that of the control and downregulated if it was less than 0.77. Based on this deduction, there were 163 upregulated proteins and 93 downregulated proteins in response to TMV (Supporting Information Table S4). Among them, 201 acetylation sites resulted in upregulation, and 124 acetylation sites resulted in downregulation (Supporting Information Figure S3a). The distribution of acetylation sites throughout the *N. benthamiana* acetylome revealed that 81% of lysine-acetylated proteins had one acetylation site, 13% had two sites, 4% had three sites, and the others had four or more sites (Supporting Information Figure S3b).

Motif Analyses and Secondary Structures of K^{ac} Proteins Differentially Expressed in Response to TMV

https://doi.org/10.1021/acsomega.2c03917
ACS Omega 2022, 7, 32496−32511

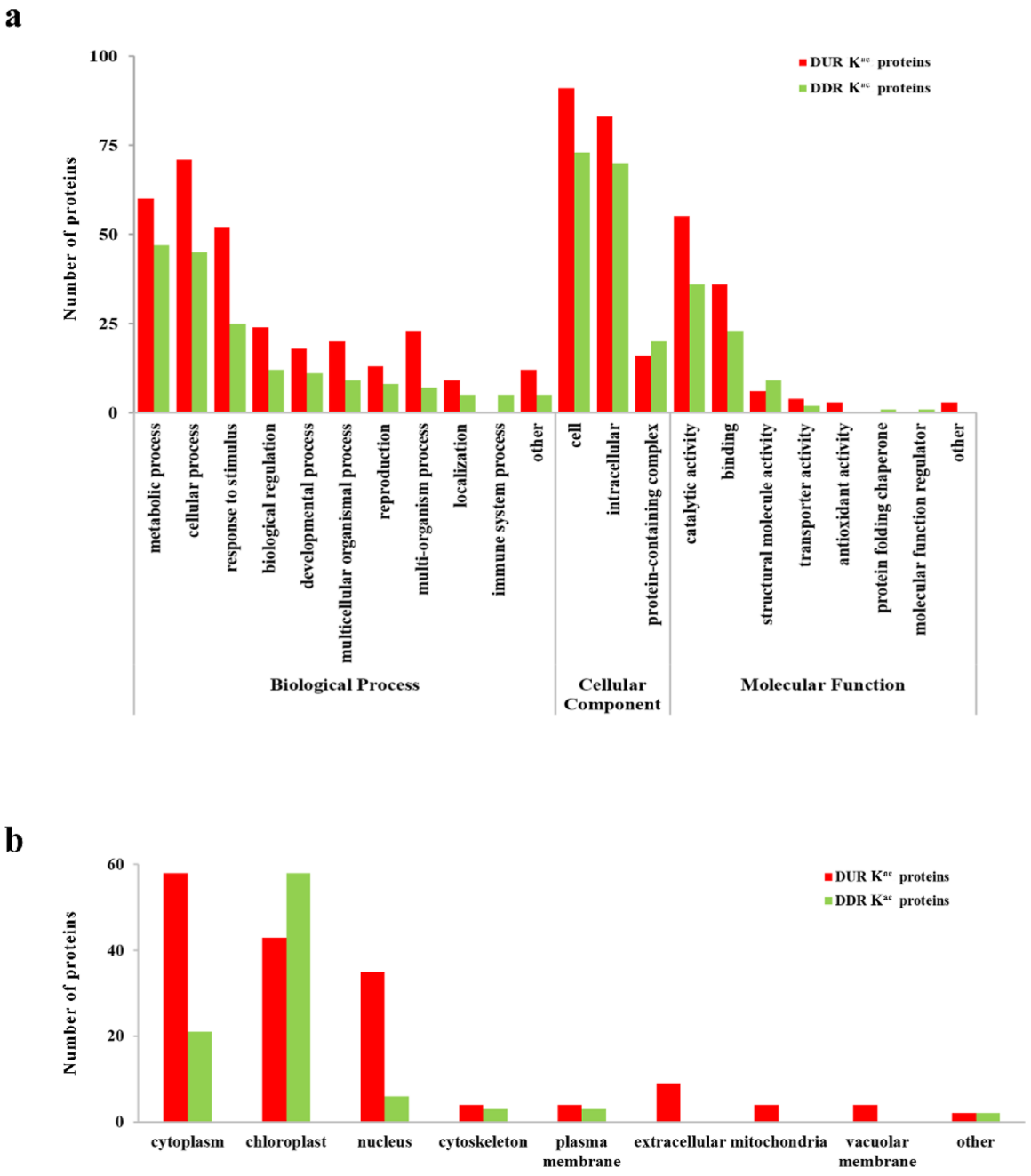

Figure 4. GO analysis and subcellular localization of lysine-acetylated proteins that are differentially expressed in response to TMV infection. (a) GO analysis of differentially expressed lysine-acetylated proteins in response to TMV infection. The red columns represent differentially upregulated (DUR) proteins, and the green columns represent differentially downregulated (DDR) proteins. (b) Subcellular localization of differentially expressed lysine-acetylated proteins in response to TMV infection.

Infection. To represent the features of K^{ac} sites of proteins in *N. benthamiana* in response to TMV, the sequence motifs around the acetylated sites were analyzed using Motif-X software. A total of 20 conserved K^{ac} site motifs were significantly enriched, including $A_{-2}/_{-1}K^{ac}K_{+1}$, $K_{-8}/_{-7}K^{ac}R_{+1}$, $E_{-3}K^{ac}K_{+1}$, $K^{ac}A_{+1}K_{+2}$, $K^{ac}K_{+1}/_{+2}/_{+3}$, $K_{-4}K^{ac}$, $K^{ac}R_{+1}/_{+2}/_{+3}$, $K^{ac}S_{+1}$, $K^{ac}N_{+1}$, $K^{ac}T_{+1}$, $K^{ac}H_{+1}$, $K^{ac}F_{+1}$, $K^{ac}D_{+2}$, and $K^{ac}E_{+2}$ (Figure 3a and Supporting Information Table S5-1). These motifs represent three different types: nonpolar types, for example, alanine (A) and phenylalanine (F); polar types that contain an uncharged residue, such as serine (S), asparagine (N), or threonine (T); and polar types that contain a charged residue, such as lysine (K), histidine (H), glutamic acid (E), arginine (R), or aspartic acid (D). The majority of conserved residues were located at the +1 or +2 positions of the K^{ac} sites, which has also been reported in humans, microbes, and plants.[17,57−59] In addition, these motifs were present in different amounts, with the $K^{ac}K_{+1}$, $K^{ac}R_{+1}$, $K^{ac}K_{+2}$, and $K^{ac}R_{+2}$ motifs being the most frequent and accounting for 14.3, 13.8, 11.7, and 9.4% of the acetylated peptides, respectively (Figure 3b and Supporting Information Table S5-1). According to Table S5-2, the positions of K ranged from −10 to −6 and from +1 to +10, especially at the −10 to −6, +1, +2, and +5 positions, and R was enriched at the −9 to −6 and +1 to +3 positions. Moreover, residues of N at +1 and T at −1 exhibited a higher frequency around the K^{ac} sites in *N.*

https://doi.org/10.1021/acsomega.2c03917
ACS Omega 2022, 7, 32496−32511

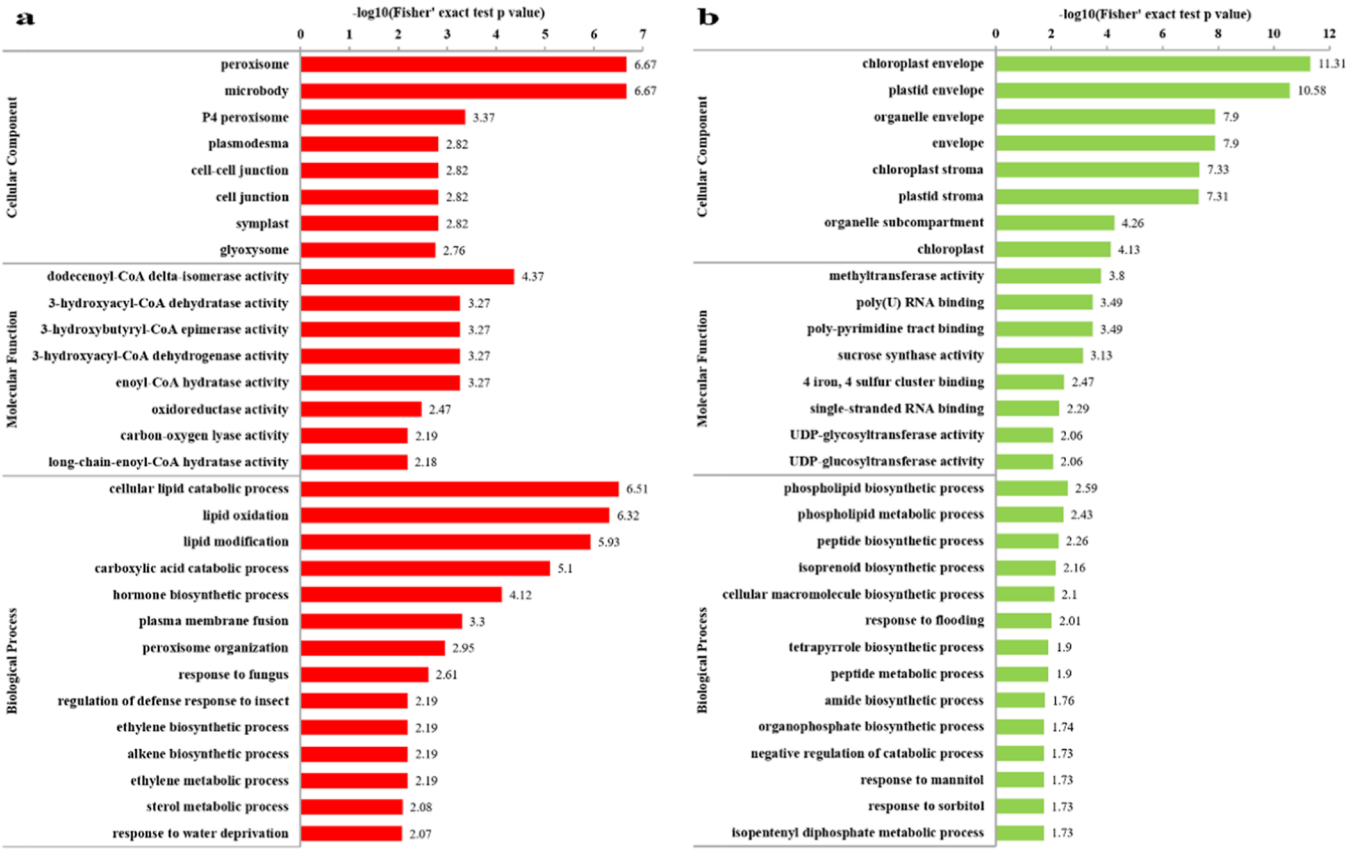

Figure 5. GO-based enrichment analysis of acetylated proteins that were differentially expressed in response to TMV. (a) Analysis of upregulated proteins in terms of biological processes, molecular functions, and cellular components. (b) Analysis of downregulated proteins in terms of biological processes, molecular functions, and cellular components.

benthamiana proteins (Figure 6b). As shown in Figure 3c, 31.2% of the acetylated sites were located in alpha-helices, and 6.1% were located in beta-strands. There were 62.7% of the acetylated sites distributed in unstructured regions of the proteins. This indicated that there was no tendency with respect to K^{ac} in *N. benthamiana* leaves between modified and nonmodified K. In addition, the surface accessibility results indicated a minor decrease in the accessibility of acetylated lysine residues compared with non-acetylated lysine residues (Figure 3d). Therefore, K^{ac} had little effect on the surface properties of proteins.

Functional Annotation and Cellular Localization of Acetylated Proteins. To comprehensively understand the acetylomics in *N. benthamiana*, GO functional annotation of differentially expressed lysine-acetylated proteins in response to infection by TMV was performed (Figure 4). The biological process results showed that 71, 60, and 52 upregulated lysine-acetylated proteins and 45, 47, and 25 downregulated lysine-acetylated proteins were classified as being associated with cellular processes, metabolic processes, and responses to stimuli, respectively, followed by biological regulation, multi-organism processes, multicellular organismal processes, and developmental processes. As for the cellular component category, lysine-acetylated proteins were distributed within the cell, intracellular, and in protein-containing complexes. The molecular function classification results showed that most of the modified proteins were connected with catalytic activity, binding function, and transporter activity (Figure 4a). The result of subcellular localization analysis indicated that the expression of 58 cytoplasmic lysine-acetylated proteins, 43 chloroplast lysine-acetylated proteins, 35 nuclear lysine-acetylated proteins, 4 cytoskeletal lysine-acetylated proteins, and 4 plasma membrane lysine-acetylated proteins was differentially upregulated, and that of 21, 58, 6, 3, and 3 of these proteins was differentially downregulated, respectively (Figure 4b). GO functional classification analysis suggested that the differentially expressed acetylated proteins are involved in a wide range of various important biological processes in *N. benthamiana*.

Functional Enrichment Analysis. For the purpose of better understanding the preferred targets for K^{ac}, functional enrichment of lysine-acetylated proteins was studied by GO functional enrichment, KEGG pathway, and protein domain analyses (Figures 5 and 6). GO enrichment analysis (Supporting Information Table S6-1) based on the biological process category revealed that upregulated differentially expressed proteins (Figure 5a) were mainly related to the cellular lipid catabolic process, lipid oxidation, and lipid modification, while downregulated differentially expressed proteins (Figure 5b) were mainly associated with the phospholipid biosynthetic process, the phospholipid metabolic process, and the peptide biosynthetic process. Most of the upregulated differentially expressed proteins in the molecular function category were related to dodecanoyl-coenzyme A (CoA) delta-isomerase activity, 3-hydroxyacyl-CoA dehydratase activity, 3-hydroxybutyryl-CoA epimerase activity, and 3-hydroxyacyl-CoA dehydrogenase activity, and the down-regulated differentially expressed proteins were associated

https://doi.org/10.1021/acsomega.2c03917
ACS Omega 2022, 7, 32496−32511

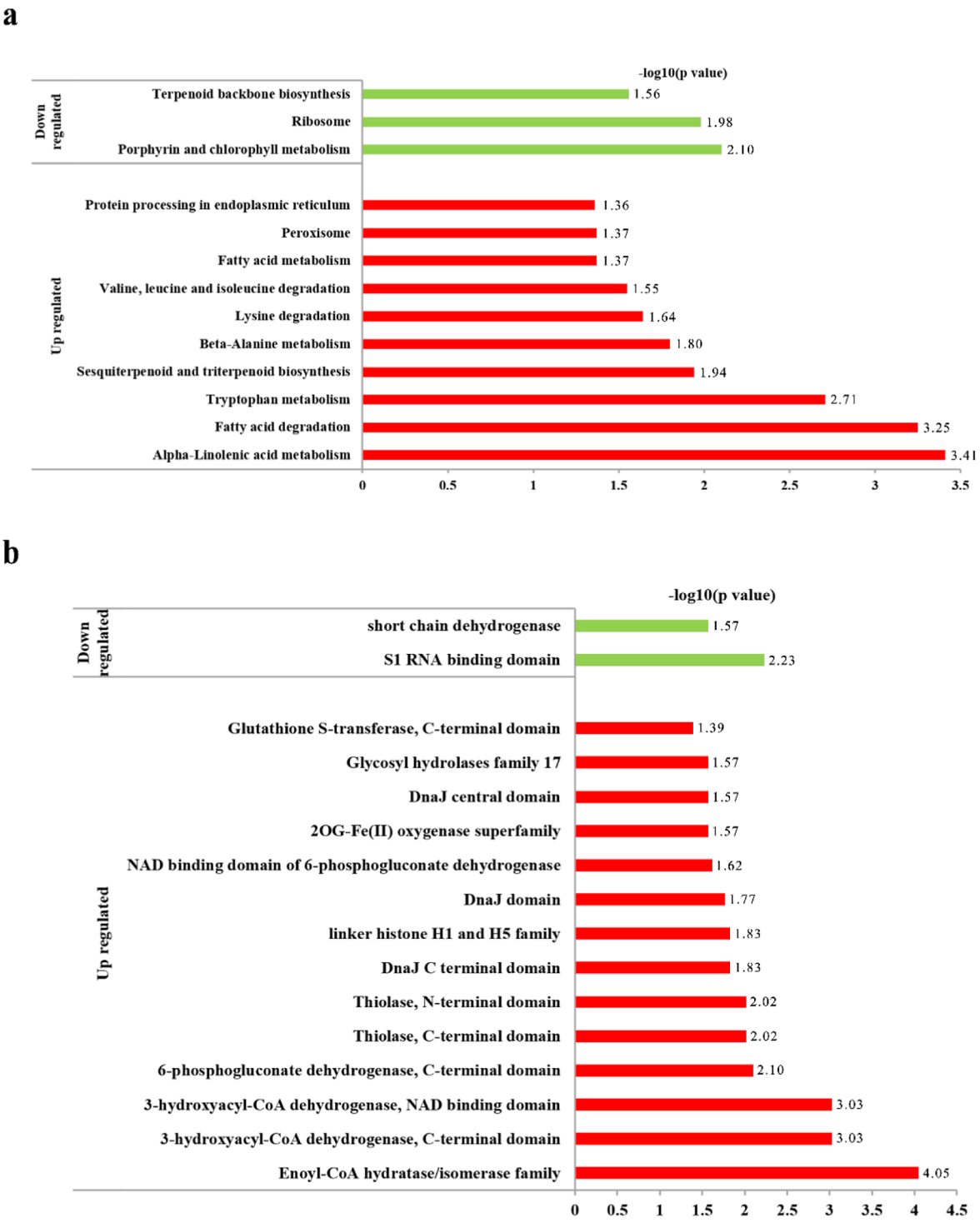

Figure 6. KEGG pathway-based analysis and protein domain enrichment analysis of acetylated proteins that were differentially expressed in response to TMV. (a) KEGG pathway-based enrichment analysis. (b) Protein domain enrichment analysis.

with methyltransferase activity, poly-pyrimidine tract binding, and poly-(U) RNA binding. The analysis of the cellular component category suggested that the expression of proteins located in peroxisomes and microbodies was mostly DUR, and a majority of the downregulated differentially expressed proteins were related to the chloroplast envelope and plastid envelope.

We conducted KEGG enrichment analysis to determine the functions of acetylated proteins in *N. benthamiana* (Figure 6a and Supporting Information Table S6-2). The expression of most of the acetylated proteins was DUR, and these proteins were involved in alpha-linolenic acid metabolism, fatty acid degradation, and tryptophan metabolism. Protein domain enrichment results showed that the upregulated differentially expressed proteins contained enoyl-CoA hydratase/isomerase family, C-terminal, 3-hydroxyacyl-CoA dehydrogenase, and NAD-binding domains and that the downregulated differentially expressed proteins contained S1 RNA binding and short-chain dehydrogenase domains (Figure 6b and Supporting Information Table S6-3). Acetylated proteins with these

https://doi.org/10.1021/acsomega.2c03917
ACS Omega 2022, 7, 32496−32511

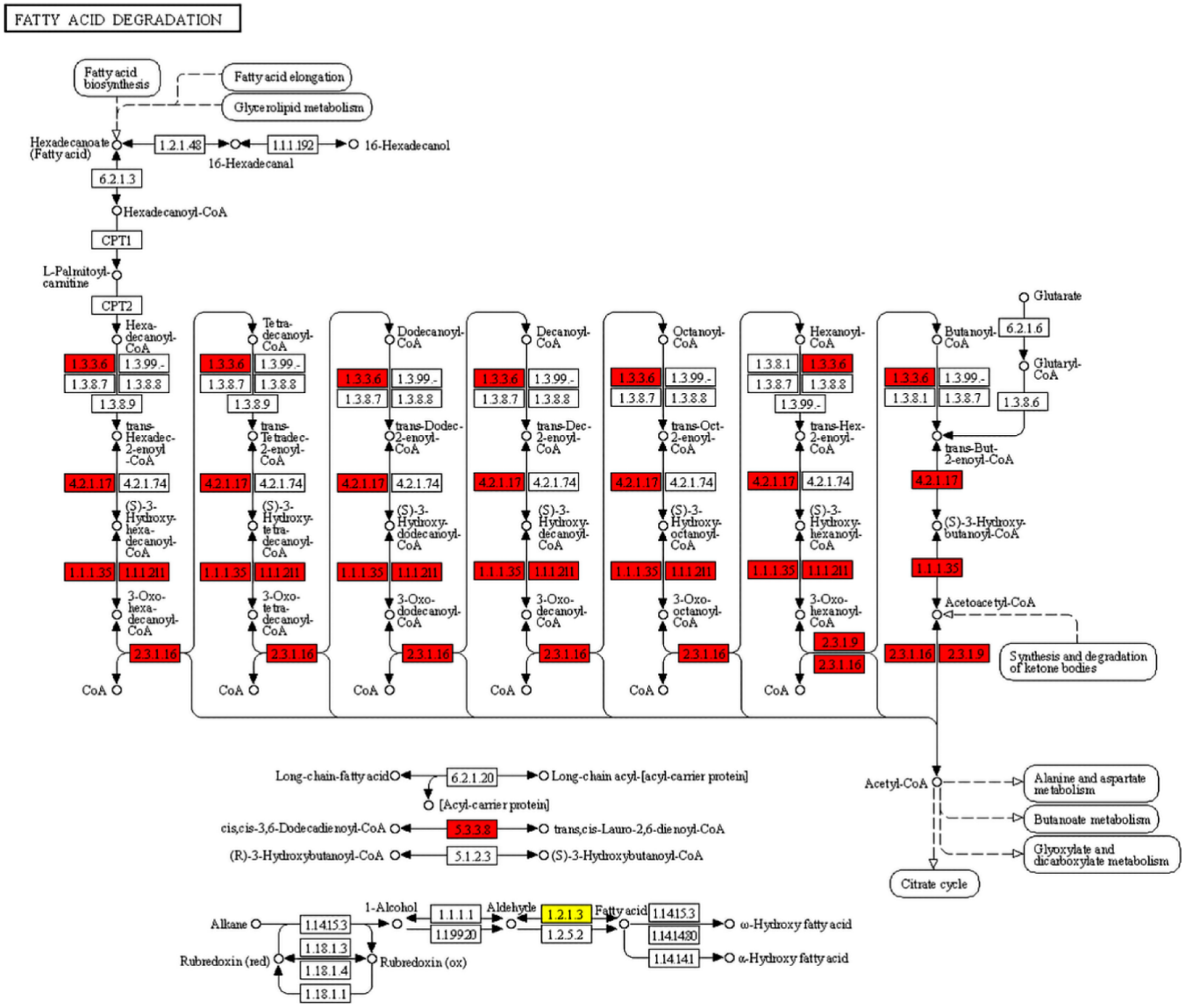

Figure 7. Lysine-acetylated proteins involved in fatty acid degradation. The red columns represent upregulated differentially expressed proteins. The yellow columns represent proteins whose expression could be DUR and DDR.

functional domains played an essential role in metabolic pathways.

Analysis of Acetylated Proteins Involved in Metabolic Pathways. Previous reports of acetylation have indicated that acetylated proteins play essential regulatory parts in multiple organisms.[1,60] The results of the GO functional, KEGG pathway, and protein domain enrichment analyses suggest that K^{ac} may be important in fatty acid degradation. Several lysine-acetylated proteins were identified as being involved in fatty acid degradation (Figure 7). LC−MS/MS analysis showed that eight fatty acid metabolism-associated enzymes were acetylated, namely, acyl-CoA oxidase, 3-hydroxyacyl-CoA dehydrogenase, long-chain 3-hydroxyacyl-CoA dehydrogenase, enoyl-CoA hydratase, acetyl-CoA acyltransferase, acetyl-CoA C-acetyltransferase, enoyl-CoA isomerase, and aldehyde dehydrogenase (NAD+).

In plants, fatty acids are widely distributed, exist in various forms, are abundant, and have important physiological functions. Fatty acids are composed of carboxylic acids attached to hydrocarbon chains[61] and are both the main components of cellular membranes and an essential source of energy. Fatty acids are also used as signal transduction mediators. In higher plants, fatty acid degradation occurs in the peroxisome, which is a distinct subcellular compartment.[62] According to the results of GO enrichment analysis, most of the upregulated differentially expressed proteins were located in peroxisomes and microbodies (Figure 5a). In fact, fatty acid degradation is an oxidative process, which includes alpha-oxidation, beta-oxidation, in-chain oxidation, and ω-oxidation. Fatty acid degradation occurs when fatty acids are catabolized to generate energy.

The enzymes associated with fatty acid degradation in higher plants are present in the peroxisome; these enzymes catalyze the basic reactions of beta-oxidation. Eight acetylated enzymes were involved in fatty acid degradation (Figure 7). Among these enzymes, five were associated with beta-oxidation,[62] which is one of the most frequently used pathways for fatty acid degradation: enoyl-CoA hydratase [EC: 4.2.1.17], acyl-CoA oxidase [EC: 1.3.3.6], acetyl-CoA acyltransferase [EC: 2.3.1.16], 3-hydroxyacyl-CoA dehydrogenase [EC: 1.1.1.35],

https://doi.org/10.1021/acsomega.2c03917
ACS Omega 2022, 7, 32496−32511

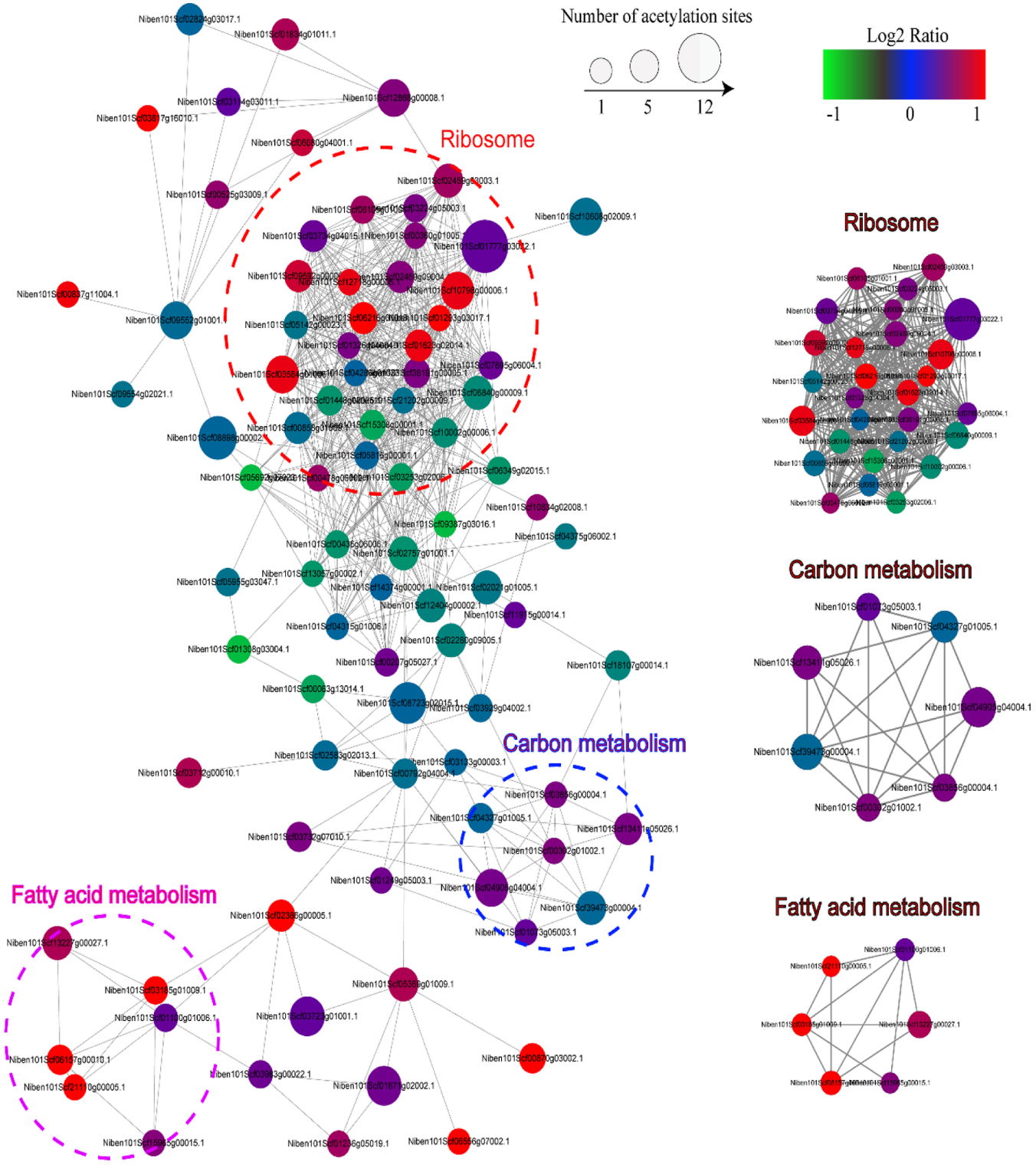

Figure 8. PPI network of newly identified acetylated proteins in *N. benthamiana*. The K^{ac} proteins were grouped using the PPI network via Cytoscape software and the STRING database. The black line represents the interaction relationship, and the circle represents the distinct biological or metabolic process.

and enoyl-CoA isomerase [EC: 5.3.3.8]. We also found four acetylated enzymes that are involved in alpha-linolenic acid metabolism (Supporting Information Figure S4): allene oxide cyclase [EC: 5.3.99.6], acyl-CoA oxidase (ACX) [EC: 1.3.3.6], enoyl-CoA hydratase/3-hydroxyacyl-CoA dehydrogenase (MFP2) [EC: 4.2.1.17, 1.1.1.35, 1.1.1.211], and acetyl-CoA acyltransferase [EC: 2.3.1.16]. Acyl-CoA oxidase catalyzes the oxidation of acyl-CoA to 2-trans-enoyl-CoA, which is the first step of the peroxisomal beta-oxidation reaction.[63] Plant acyl-CoA oxidase is considered to be a flavin adenine dinucleotide (FAD)-containing protein. FAD-containing proteins, nicotinamide adenine dinucleotide (NADH), and adenosine triphosphate (ATP) are involved in many biological processes.[64] The second step in fatty acid beta-oxidation is catalyzed by enoyl-

https://doi.org/10.1021/acsomega.2c03917
ACS Omega 2022, 7, 32496−32511

CoA hydratase.[65] 3-Hydroxyacyl-CoA dehydrogenase is considered as an oxidoreductase; this enzyme catalyzes the third step of beta-oxidation.[66] Acetyl-CoA acyltransferase, which is found in both eukaryotes and prokaryotes, acts on 3-oxoacyl-CoA to generate acetyl-CoA and an acyl-CoA shortened by two carbon atoms.[67] Enoyl-CoA isomerase catalyzes the conversion of cis or trans double bonds of CoA-bound fatty acids at the gamma-carbon to trans double bonds at the beta-carbon; it is important in the metabolism of unsaturated fatty acids in beta-oxidation.[68,69] The core process of energy production involves the oxidation of acetyl-CoA to CO_2 through the tricarboxylic acid cycle,[70] so acetylation of *N. benthamiana* plays an important role in energy metabolism. 12-Oxo-phytodienoic acid (12-OPDA) is catalyzed by OPDA reductase (OPR) to produce OPC8. OPC8-CoA is formed under the action of OPC-CoA ligase on OPC8. Through three beta-oxidation reactions, OPC8 is ultimately oxidized to jasmonic acid (JA). In summary, these results indicate that K^{ac} affects important enzymes involved in fatty acid degradation and alpha-linolenic acid metabolic pathways in *N. benthamiana*.

PPI Network Analysis. To further understand how acetylation regulates the cellular and metabolic processes of *N. benthamiana* in response to TMV stress, we constructed a PPI network using Cytoscape software and the STRING database. The results from the MCODE plug-in toolkit mapped a total of 88 acetylated proteins (Figure 8 and Supporting Information Table S7), which stands for a comprehensive sight of how acetylated proteins perform multiple functions in *N. benthamiana*. The top three clusters were "ribosome", "carbon metabolism", and "fatty acid metabolism". The complex interaction among acetylated proteins indicates the possibility of their coordination in response to TMV stress.

PRM-Based Validation and Software Prediction. A PRM assay was conducted to verify acetylome results. Depending on the above analysis, we selected eight peptides to evaluate their involvement in important physiological processes, and the ratio of acetylation abundance varied widely. The results of five peptide PRMs and label-free quantification were essentially consistent, indicating that the whole-cell proteome results were robust (Supporting Information Table S8). According to the fold change (TMV/PBS) in Supporting Information Table S8, we chose peroxisomal acyl-CoA oxidase 1 and 3-ketoacyl-CoA thiolase for additional verification. PAIL (v.1.0) software was used to predict the acetylated sites in these proteins. The result showed that there were 15 and 20 acetylation sites on 3-ketoacyl-CoA thiolase and peroxisomal acyl-coenzyme A oxidase 1, respectively. Among them, the acetylation site at K44 on 3-ketoacyl-CoA thiolase and the acetylation site at K449 on peroxisomal acyl-coenzyme A oxidase 1 (Supporting Information Table S9) were consistent with the result of differentially expressed lysine-acetylated proteins (Supporting Information Table S4).

DISCUSSION

K^{ac} is a dynamic and reversible PTM of proteins that widely occurs in prokaryotes and eukaryotes. Recently, an increasing number of plant acetylomes have been reported, including those of *Arabidopsis thaliana*, *Oryza sativa*, *Triticum aestivum*, *Zea mays*, *Glycine max*, *Solanum tuberosum*, *Vitis vinifera*, and *P. tomentosa*.[1,7,8,17,25,26,71,72] According to molecular experiments, we found that TMV infection could induce alterations in acetylation levels. The changes in TMV replication expression in *N. benthamiana* and acetylation levels had the same tendency. We also found that the level of TMV replication expression and acetylation in NAM-treated plants was upregulated. According to previous research reports, pathogen infection can change the acetylation level of host plants and favor pathogen infection. For example, fungal pathogens promote susceptibility in soybean and maize through altering protein acetylation.[29] In cauliflower mosaic virus (CaMV) infection plants, the global levels of histone acetylation are increased, and the infection of CAMV is promoted.[73] However, to date, changes in acetylation levels after TMV infection have seldom been reported. The acetylated proteins identified in our putative study may be involved in the pathogenic process of viral infection. To validate this hypothesis, we combined proteomic and acetylomic studies of K^{ac} in *N. benthamiana* and provided global views into the functions of proteins in different processes following treatment with TMV. We identified that 256 regulated proteins were screened based on the fold-change threshold, which were responding to viral infection in this study (Supporting Information Figure S4b).

Some motifs of *N. benthamiana* proteins have been reported in other species, such as $K^{ac}H_{+1}$ and $K^{ac}R_{+2}$ in humans;[59] $K^{ac}H_{+1}$ and $K^{ac}F_{+1}$ in strawberry, common wheat, and *O. sativa*;[1,12,26] and $K^{ac}S_{+1}$, $K^{ac}R_{+1/+2}$, $K^{ac}H_{+1}$, $K^{ac}N_{+1}$, $K^{ac}K_{+1/+2}$, $K^{ac}D_{+2}$, $K^{ac}E_{+2}$, $K^{ac}T_{+1}$, and $E_{-3}K^{ac}K_{+1}$ in *Trichinella spiralis* and tea.[45,58] These results indicated that K^{ac} is also a kind of conserved PTM between *N. benthamiana* and various species. As a type of PTM, K^{ac} exhibits an important capability in regulating protein functions,[14] such as regulating energy metabolism and crucial metabolic pathways that react to biotic and abiotic stresses.[27,74] In *P. tomentosa*, researchers revealed several acetylation sites on ribulose bisphosphate carboxylase oxygenase and protochlorophyllide after phytoplasma infection, which play prominent roles in starch and chlorophyll synthesis.[40] We revealed that 101 and 79 acetylated proteins were localized in the chloroplast and cytoplasm, respectively, in *N. benthamiana* (Figure 7b), and many of them are involved in carbon metabolism and fatty acid metabolism.

Fatty acids are significant and essential elements of plant cells that can provide structural integrity, metabolic energy, and signal transduction functionality.[75] More and more studies have indicated that fatty acids and their derivatives modulate normal and disease-related physiology in plants, which means that fatty acid metabolism is one of the most vital metabolic processes. Increasing amounts of research also indicate that fatty acids and their derivatives can act as signaling molecules that modulate normal and disease-related physiology in plants. For example, oleic acid and linoleic acid induce the activation of NADPH oxidase, which participates in the production of reactive oxygen species (ROS).[76] Among phytohormones, salicylic acid (SA) and JA are related to the regulation of plant defense. It has also been shown that methyl jasmonate (MeJA) and methyl salicylate (MeSA) are necessary for the systemic resistance response against TMV.[77] In particular, JA is derived from alpha-linolenic acid.[75] JA is involved in both induced system resistance (ISR) and systemic acquired resistance (SAR), and the signaling mediated by JA is vital in plant defense against biotic and abiotic stresses.[78] JA and its volatile methyl ester (MeJA) are widespread within the plant kingdom. Prior research has reported that JA and MeJA can regulate SA

https://doi.org/10.1021/acsomega.2c03917
ACS Omega 2022, 7, 32496−32511

and MeSA production, respectively; these four metabolites take part in the systemic resistance response against TMV.[77]

In this study, eight proteins were involved in fatty acid degradation pathways, and four proteins were associated with alpha-linolenic acid metabolic pathways (Supporting Information Table S6). The acetylation level of these proteins increased, and PRM verification indicated the presence of modification sites related to fatty acid degradation and alpha-linolenic acid metabolism. Because alpha-linolenic acid is also a type of fatty acid, it is suggested that changes in the acetylation levels of proteins in fatty acid metabolism may be associated with the immune response to TMV in *N. benthamiana*. There are few reports on the relationship between fatty acids and antivirals in plants. However, the fatty acid synthesis pathway is the key factor for syndrome coronavirus 2 (SARS-CoV-2) rapid replication in mouse cells. Fatty acid synthesis inhibitors have broad-spectrum antiviral activity against SARS-CoV-2.[79] In ovarian granulosa cells of polycystic ovary syndrome, differentially acetylated proteins were significantly enriched in the metabolic pathways of glycolysis, fatty acid degradation, TCA cycle, and other metabolic processes.[80] Based on the above research, we speculate that the key proteins in the fatty acid degradation pathway are acetylated in response to TMV infection, which affects the normal metabolic process of fatty acids in *N. benthamiana* and then affects the production of antiviral active substances, thus promoting the replication and infection of the virus. However, further studies are needed to validate the function of acetylated proteins and their interactions with plant proteins. According to the prediction results of protein acetylation sites combined with acetylation modification omics data, we will select peroxisomal acyl-CoA oxidase 1 and 3-ketoacyl-CoA thiolase for additional verification and carry out additional in-depth research.

CONCLUSIONS

In this study, validation assays showed that TMV infection resulted in altered K^{ac} levels and that K^{ac} may contribute to viral infection. We utilized proteomic and acetylomic methods to investigate modifications in protein abundance and K^{ac} in TMV-infected *N. benthamiana* seedlings. We identified 2082 acetylation sites on 1319 proteins from seedling leaves. Characterization of the acetylated proteins shows that acetylation plays a crucial role in numerous cellular processes, especially fatty acid degradation and alpha-linolenic acid metabolic pathways, which are involved in energy metabolism and plant disease resistance. PRM confirmed the presence of acetylation sites. Together, our analysis provides a comprehensive view of K^{ac} in TMV-infected *N. benthamiana* seedlings. These results might offer a beneficial reference for future studies on the essential role of K^{ac} in *N. benthamiana* and other plant species in response to TMV infection or other pathogenic infections.

ASSOCIATED CONTENT

Supporting Information

The Supporting Information is available free of charge at https://pubs.acs.org/doi/10.1021/acsomega.2c03917.

Detailed information of all the quantified proteins (three replicates each); detailed information of differentially expressed proteins; information on the identified lysine-acetylated proteins (three replicates each); detailed information concerning differentially expressed lysine-acetylated proteins; motifs of lysine-acetylated peptides; frequency of the different types of aa around acetylated lysine residues; GO-based enrichment analysis of acetylated proteins; KEGG pathway analysis of acetylated proteins; protein domain enrichment analysis of acetylated proteins; PPI network information; PRM assay results for verification of the acetylome results; acetylation sites prediction results of proteins; proteome-wide identification of lysine-acetylated proteins in *N. benthamiana*; functional classification of proteins that were differentially expressed in response to TMV infection; identification of lysine-acetylated proteins and sites in *N. benthamiana*; and lysine-acetylated proteins involved in alpha-linolenic acid metabolism (PDF)

Cross-talk of protein expression and lysine acetylation in response to TMV infection in Nicotiana benthamiana- (XLSX)

AUTHOR INFORMATION

Corresponding Authors

Fenglong Wang − *Key Laboratory of Tobacco Pest Monitoring, Controlling & Integrated Management, Tobacco Research Institute of the Chinese Academy of Agricultural Sciences, Qingdao 266101, China*; Email: wangfenglong@caas.cn

Jinguang Yang − *Key Laboratory of Tobacco Pest Monitoring, Controlling & Integrated Management, Tobacco Research Institute of the Chinese Academy of Agricultural Sciences, Qingdao 266101, China*; orcid.org/0000-0002-9584-9634; Phone: +86-532-88703236; Email: yangjinguang@caas.cn

Authors

Liyun Song − *Key Laboratory of Tobacco Pest Monitoring, Controlling & Integrated Management, Tobacco Research Institute of the Chinese Academy of Agricultural Sciences, Qingdao 266101, China*; orcid.org/0000-0002-3289-7524

Huaixu Zhan − *Key Laboratory of Tobacco Pest Monitoring, Controlling & Integrated Management, Tobacco Research Institute of the Chinese Academy of Agricultural Sciences, Qingdao 266101, China; Graduate School of Chinese Academy of Agricultural Sciences, Beijing 100081, China*

Yujie Wang − *Luoyang Branch of Henan Tobacco Company, Luoyang 471000, China*

Zhonglong Lin − *Yunnan Tobacco Company of the China National Tobacco Corporation, Kunming 650011, China*

Bin Li − *Sichuan Tobacco Company, Chengdu 610017, China*

Lili Shen − *Key Laboratory of Tobacco Pest Monitoring, Controlling & Integrated Management, Tobacco Research Institute of the Chinese Academy of Agricultural Sciences, Qingdao 266101, China*

Yubing Jiao − *Key Laboratory of Tobacco Pest Monitoring, Controlling & Integrated Management, Tobacco Research Institute of the Chinese Academy of Agricultural Sciences, Qingdao 266101, China*

Ying Li − *Key Laboratory of Tobacco Pest Monitoring, Controlling & Integrated Management, Tobacco Research Institute of the Chinese Academy of Agricultural Sciences, Qingdao 266101, China*

Complete contact information is available at:

https://pubs.acs.org/10.1021/acsomega.2c03917

Author Contributions

[#]L.S. and H.Z. have contributed equally to this work.

Notes

The authors declare no competing financial interest.

In this section, proteomics and protein acetylomics mass spectrometry data were stored through the PRIDE partner repository of the ProteomeXchange Consortium, with the data set identifiers PXD035736 and PXD035737.

■ ACKNOWLEDGMENTS

This work was supported by the China National Tobacco Corporation Green Tobacco Prevention and Control Major Special Projects (110202001033 [LS-02] and 110202101045 [LS-05]), Shandong Provincial Natural Science Foundation Project (ZR202103070049), Sichuan Tobacco Company Science and Technology Project (SCYC202008), Henan Tobacco Company Luoyang City Company Science and Technology Project (2020410300270076), and Yunnan Tobacco Company Science and Technology Project (2020530000241011).

■ REFERENCES

(1) Zhang, Y.; Song, L.; Liang, W.; Mu, P.; Wang, S.; Lin, Q. Comprehensive profiling of lysine acetylproteome analysis reveals diverse functions of lysine acetylation in common wheat. *Sci. Rep.* **2016**, *6*, 21069.

(2) Venne, A. S.; Zahedi, R. P. The potential of fractional diagonal chromatography strategies for the enrichment of post-translational modifications. *EuPA Open Proteomics* **2014**, *4*, 165−170.

(3) Zhan, H.; Song, L.; Kamran, A.; Han, F.; Li, B.; Zhou, Z.; Liu, T.; Shen, L.; Li, Y.; Wang, F.; Yang, J. Comprehensive proteomic analysis of lysine ubiquitination in seedling leaves of *Nicotiana tabacum*. *ACS Omega* **2020**, *5*, 20122−20133.

(4) Wolffe, A. P. Histone deacetylase: a regulator of transcription. *Science* **1996**, *272*, 371.

(5) Sabari, B. R.; Zhang, D.; Allis, C. D.; Zhao, Y. Metabolic regulation of gene expression through histone acylations. *Nat. Rev. Mol. Cell Biol.* **2017**, *18*, 90−101.

(6) Zhou, H.; Finkemeier, I.; Guan, W.; Tossounian, M. A.; Wei, B.; Young, D.; Huang, J.; Messens, J.; Yang, X.; Zhu, J.; Wilson, M. H.; Shen, W.; Xie, Y.; Foyer, C. H. Oxidative stress-triggered interactions between the succinyl- and acetyl-proteomes of rice leaves. *Plant, Cell Environ.* **2018**, *41*, 1139−1153.

(7) Walley, J. W.; Shen, Z.; McReynolds, M. R.; Schmelz, E. A.; Briggs, S. P. Fungal-induced protein hyperacetylation in maize identified by acetylome profiling. *Proc. Natl. Acad. Sci. U.S.A.* **2018**, *115*, 210−215.

(8) Nallamilli, B. R.; Edelmann, M. J.; Zhong, X.; Tan, F.; Mujahid, H.; Zhang, J.; Nanduri, B.; Peng, Z. Global analysis of lysine acetylation suggests the involvement of protein acetylation in diverse biological processes in rice (*Oryza sativa*). *PLoS One* **2014**, *9*, No. e89283.

(9) Henriksen, P.; Wagner, S. A.; Weinert, B. T.; Sharma, S.; Bačinskaja, G.; Rehman, M.; Juffer, A. H.; Walther, T. C.; Lisby, M.; Choudhary, C. Proteome-wide analysis of lysine acetylation suggests its broad regulatory scope in Saccharomyces cerevisiae. *Mol. Cell. Proteomics* **2012**, *11*, 1510−1522.

(10) Mischerikow, N.; Heck, A. J. Targeted large-scale analysis of protein acetylation. *Proteomics* **2011**, *11*, 571−589.

(11) Liu, F.; Yang, M.; Wang, X.; Yang, S.; Gu, J.; Zhou, J.; Zhang, X. E.; Deng, J.; Ge, F. Acetylome analysis reveals diverse functions of lysine acetylation in Mycobacterium tuberculosis. *Mol. Cell. Proteomics* **2014**, *13*, 3352−3366.

(12) Xue, C.; Liu, S.; Chen, C.; Zhu, J.; Yang, X.; Zhou, Y.; Guo, R.; Liu, X.; Gong, Z. Global proteome analysis links lysine acetylation to diverse functions in *Oryza sativa*. *Proteomics* **2018**, *18*, 1700036.

(13) Sterner, D. E.; Berger, S. L. Acetylation of histones and transcription-related factors. *Microbiol. Mol. Biol. Rev.* **2000**, *64*, 435−459.

(14) Guan, K. L.; Xiong, Y. Regulation of intermediary metabolism by protein acetylation. *Trends Biochem. Sci.* **2011**, *36*, 108−116.

(15) Guarente, L. The logic linking protein acetylation and metabolism. *Cell Metab.* **2011**, *14*, 151−153.

(16) Wang, Q.; Zhang, Y.; Yang, C.; Xiong, H.; Lin, Y.; Yao, J.; Li, H.; Xie, L.; Zhao, W.; Yao, Y.; Ning, Z. B.; Zeng, R.; Xiong, Y.; Guan, K. L.; Zhao, S.; Zhao, G. P. Acetylation of metabolic enzymes coordinates carbon source utilization and metabolic flux. *Science* **2010**, *327*, 1004−1007.

(17) Cao, Y.; Fan, G.; Wang, Z.; Gu, Z. Phytoplasma-induced changes in the acetylome and succinylome of paulownia tomentosa provide evidence for involvement of acetylated proteins in Witches' broom disease. *Mol. Cell. Proteomics* **2019**, *18*, 1210−1226.

(18) Sokol, A.; Kwiatkowska, A.; Jerzmanowski, A.; Prymakowska-Bosak, M. Up-regulation of stress-inducible genes in tobacco and Arabidopsis cells in response to abiotic stresses and ABA treatment correlates with dynamic changes in histone H3 and H4 modifications. *Planta* **2007**, *227*, 245−254.

(19) Kim, J. M.; To, T. K.; Ishida, J.; Morosawa, T.; Kawashima, M.; Matsui, A.; Toyoda, T.; Kimura, H.; Shinozaki, K.; Seki, M. Alterations of lysine modifications on the histone H3 N-tail under drought stress conditions in Arabidopsis thaliana. *Plant Cell Physiol.* **2008**, *49*, 1580−1588.

(20) Tsuji, H.; Saika, H.; Tsutsumi, N.; Hirai, A.; Nakazono, M. Dynamic and reversible changes in histone H3-Lys4 methylation and H3 acetylation occurring at submergence-inducible genes in rice. *Plant Cell Physiol.* **2006**, *47*, 995−1003.

(21) Choudhary, C.; Kumar, C.; Gnad, F.; Nielsen, M. L.; Rehman, M.; Walther, T. C.; Olsen, J. V.; Mann, M. Lysine acetylation targets protein complexes and co-regulates major cellular functions. *Science* **2009**, *325*, 834−840.

(22) Xiong, Y.; Guan, K. L. Mechanistic insights into the regulation of metabolic enzymes by acetylation. *J. Cell Biol.* **2012**, *198*, 155−164.

(23) Starai, V. J.; Escalante-Semerena, J. C. Identification of the protein acetyltransferase (Pat) enzyme that acetylates acetyl-CoA synthetase in Salmonella enterica. *J. Mol. Biol.* **2004**, *340*, 1005−1012.

(24) Liang, W.; Malhotra, A.; Deutscher, M. P. Acetylation regulates the stability of a bacterial protein: growth stage-dependent modification of RNase R. *Mol. Cell* **2011**, *44*, 160−166.

(25) Smith-Hammond, C. L.; Swatek, K. N.; Johnston, M. L.; Thelen, J. J.; Miernyk, J. A. Initial description of the developing soybean seed protein Lys-N(epsilon)-acetylome. *J. Proteomics* **2014**, *96*, 56−66.

(26) Fang, X.; Chen, W.; Zhao, Y.; Ruan, S.; Zhang, H.; Yan, C.; Jin, L.; Cao, L.; Zhu, J.; Ma, H.; Cheng, Z. Global analysis of lysine acetylation in strawberry leaves. *Front. Plant Sci.* **2015**, *6*, 739.

(27) Le Roux, C.; Huet, G.; Jauneau, A.; Camborde, L.; Trémousaygue, D.; Kraut, A.; Zhou, B.; Levaillant, M.; Adachi, H.; Yoshioka, H.; Raffaele, S.; Berthomé, R.; Couté, Y.; Parker, J. E.; Deslandes, L. A receptor pair with an integrated decoy converts pathogen disabling of transcription factors to immunity. *Cell* **2015**, *161*, 1074−1088.

(28) Lin, W. C.; Lu, C. F.; Wu, J. W.; Cheng, M. L.; Lin, Y. M.; Yang, N. S.; Black, L.; Green, S. K.; Wang, J. F.; Cheng, C. P. Transgenic tomato plants expressing the Arabidopsis NPR1 gene display enhanced resistance to a spectrum of fungal and bacterial diseases. *Transgenic Res.* **2004**, *13*, 567−581.

(29) Kong, L.; Qiu, X.; Kang, J.; Wang, Y.; Chen, H.; Huang, J.; Qiu, M.; Zhao, Y.; Kong, G.; Ma, Z.; Wang, Y.; Ye, W.; Dong, S.; Ma, W.; Wang, Y. A phytophthora effector manipulates host histone acetylation and reprograms defense gene expression to promote infection. *Curr. Biol.* **2017**, *27*, 981−991.

(30) Ding, B.; Bellizzi, R. B.; Ning, Y.; Meyers, B. C.; Wang, G. L. HDT701, a histone H4 deacetylase, negatively regulates plant innate immunity by modulating histone H4 acetylation of defense-related genes in rice. *Plant Cell* **2012**, *24*, 3783−3794.
(31) Sun, X.; Li, Z.; Liu, H.; Yang, J.; Liang, W.; Peng, Y. L.; Huang, J. Large-scale identification of lysine acetylated proteins in vegetative hyphae of the rice blast fungus. *Sci. Rep.* **2017**, *7*, 15316.
(32) Tasset, C.; Bernoux, M.; Jauneau, A.; Pouzet, C.; Brière, C.; Kieffer-Jacquinod, S.; Rivas, S.; Marco, Y.; Deslandes, L. Autoacetylation of the *Ralstonia solanacearum* effector PopP2 targets a lysine residue essential for RRS1-R-mediated immunity in Arabidopsis. *PLoS Pathog.* **2010**, *6*, No. e1001202.
(33) Lv, B.; Yang, Q.; Li, D.; Liang, W.; Song, L. Proteome-wide analysis of lysine acetylation in the plant pathogen Botrytis cinerea. *Sci. Rep.* **2016**, *6*, 29313.
(34) Zhou, S.; Yang, Q.; Yin, C.; Liu, L.; Liang, W. Systematic analysis of the lysine acetylome in *Fusarium graminearum*. *BMC Genom.* **2016**, *17*, 1019.
(35) Ding, S. L.; Liu, W.; Iliuk, A.; Ribot, C.; Vallet, J.; Tao, A.; Wang, Y.; Lebrun, M. H.; Xu, J. R. The tig1 histone deacetylase complex regulates infectious growth in the rice blast fungus Magnaporthe oryzae. *Plant Cell* **2010**, *22*, 2495−2508.
(36) Kim, D.; Yu, B. J.; Kim, J. A.; Lee, Y. J.; Choi, S. G.; Kang, S.; Pan, J. G. The acetylproteome of Gram-positive model bacterium Bacillus subtilis. *Proteomics* **2013**, *13*, 1726−1736.
(37) Lee, D. W.; Kim, D.; Lee, Y. J.; Kim, J. A.; Choi, J. Y.; Kang, S.; Pan, J. G. Proteomic analysis of acetylation in thermophilic Geobacillus kaustophilus. *Proteomics* **2013**, *13*, 2278−2282.
(38) Liu, L.; Wang, G.; Song, L.; Lv, B.; Liang, W. Acetylome analysis reveals the involvement of lysine acetylation in biosynthesis of antibiotics in Bacillus amyloliquefaciens. *Sci. Rep.* **2016**, *6*, 20108.
(39) Liao, G.; Xie, L.; Li, X.; Cheng, Z.; Xie, J. Unexpected extensive lysine acetylation in the trump-card antibiotic producer Streptomyces roseosporus revealed by proteome-wide profiling. *J. Proteomics* **2014**, *106*, 260−269.
(40) Cao, Y.; Guoqiang, F.; Zhe, W.; Zhibin, G. Phytoplasma-induced changes in the acetylome and succinylome of Paulownia tomentosa provide evidence for involvement of acetylated proteins in witches' broom disease. *Mol. Cell. Proteomics* **2019**, *18*, 1210.
(41) Xu, J.; Xu, H.; Liu, Y.; Wang, X.; Xu, Q.; Deng, X. Genome-wide identification of sweet orange (Citrus sinensis) histone modification gene families and their expression analysis during the fruit development and fruit-blue mold infection process. *Front. Plant Sci.* **2015**, *6*, 607.
(42) Ding, B.; Bellizzi, M. d. R.; Ning, Y.; Meyers, B. C.; Wang, G.-L. HDT701, a histone H4 deacetylase, negatively regulates plant innate immunity by modulating histone H4 acetylation of defense-related genes in rice. *Plant Cell.* **2012**, *24*, 3783.
(43) Xing, G.; Jin, M.; Qu, R.; Zhang, J.; Han, Y.; Han, Y.; Wang, X.; Li, X.; Ma, F.; Zhao, X. Genome-wide investigation of histone acetyltransferase gene family and its responses to biotic and abiotic stress in foxtail millet (Setaria italica [L.] P. Beauv). *BMC Plant Biol.* **2022**, *22*, 292.
(44) Qin, Y.; Wang, J.; Wang, F.; Shen, L.; Zhou, H.; Sun, H.; Hao, K.; Song, L.; Zhou, Z.; Zhang, C.; Wu, Y.; Yang, J. Purification and characterization of a secretory alkaline metalloprotease with highly potent antiviral activity from Serratia marcescens strain S3. *J. Agric. Food Chem.* **2019**, *67*, 3168−3178.
(45) Jiang, J.; Gai, Z.; Wang, Y.; Fan, K.; Sun, L.; Wang, H.; Ding, Z. Comprehensive proteome analyses of lysine acetylation in tea leaves by sensing nitrogen nutrition. *BMC Genom.* **2018**, *19*, 840.
(46) Dimmer, E. C.; Huntley, R. P.; Alam-Faruque, Y.; Sawford, T.; O'Donovan, C.; Martin, M. J.; Bely, B.; Browne, P.; Mun Chan, W.; Eberhardt, R.; Gardner, M.; Laiho, K.; Legge, D.; Magrane, M.; Pichler, K.; Poggioli, D.; Sehra, H.; Auchincloss, A.; Axelsen, K.; Blatter, M. C.; Boutet, E.; Braconi-Quintaje, S.; Breuza, L.; Bridge, A.; Coudert, E.; Estreicher, A.; Famiglietti, L.; Ferro-Rojas, S.; Feuermann, M.; Gos, A.; Gruaz-Gumowski, N.; Hinz, U.; Hulo, C.; James, J.; Jimenez, S.; Jungo, F.; Keller, G.; Lemercier, P.; Lieberherr, D.; Masson, P.; Moinat, M.; Pedruzzi, I.; Poux, S.; Rivoire, C.; Roechert, B.; Schneider, M.; Stutz, A.; Sundaram, S.; Tognolli, M.; Bougueleret, L.; Argoud-Puy, G.; Cusin, I.; Duek- Roggli, P.; Xenarios, I.; Apweiler, R. The UniProt-GO annotation database in 2011. *Nucleic Acids Res.* **2012**, *40*, D565−D570.
(47) Moriya, Y.; Masumi, I.; Shujiro, O.; Yoshizawa, A. C.; Minoru, K. KAAS: an automatic genome annotation and pathway reconstruction server. *Nucleic Acids Res.* **2007**, *35*, W182−W185.
(48) Horton, P.; Park, K. J.; Obayashi, T.; Fujita, N.; Harada, H.; Adams-Collier, C. J.; Nakai, K. WoLF PSORT: protein localization predictor. *Nucleic Acids Res.* **2007**, *35*, W585−W587.
(49) Zheng, X.; Yang, Q.; Zhao, L.; Apaliya, M. T.; Zhang, X.; Zhang, H. Crosstalk between proteins expression and lysine acetylation in response to patulin stress in Rhodotorula mucilaginosa. *Sci. Rep.* **2017**, *7*, 13490.
(50) Petersen, B.; Petersen, T. N.; Andersen, P.; Nielsen, M.; Lundegaard, C. A generic method for assignment of reliability scores applied to solvent accessibility predictions. *BMC Struct. Biol.* **2009**, *9*, 51.
(51) Jiao, X.; Sherman, B. T.; Huang, W.; Stephens, R.; Baseler, M. W.; Lane, H. C.; Lempicki, R. A. DAVID-WS: a stateful web service to facilitate gene/protein list analysis. *Bioinformatics* **2012**, *28*, 1805−1806.
(52) Doerks, T.; Copley, R. R.; Schultz, J.; Ponting, C. P.; Bork, P. Systematic identification of novel protein domain families associated with nuclear functions. *Genome Res.* **2002**, *12*, 47−56.
(53) Shannon, P.; Markiel, A.; Ozier, O.; Baliga, N. S.; Wang, J. T.; Ramage, D.; Amin, N.; Schwikowski, B.; Ideker, T. Cytoscape: a software environment for integrated models of biomolecular interaction networks. *Genome Res.* **2003**, *13*, 2498−2504.
(54) Bader, G. D.; Hogue, C. W. An automated method for finding molecular complexes in large protein interaction networks. *BMC Bioinf.* **2003**, *4*, 2.
(55) Gao, X.; Hong, H.; Li, W. C.; Yang, L.; Huang, J.; Xiao, Y. L.; Chen, X. Y.; Chen, G. Y. Downregulation of rubisco activity by non-enzymatic acetylation of RbcL. *Mol. Plant* **2016**, *9*, 1018−1027.
(56) Scott, I. Regulation of cellular homoeostasis by reversible lysine acetylation. *Essays Biochem.* **2012**, *52*, 13−22.
(57) Xiong, Y.; Peng, X.; Cheng, Z.; Liu, W.; Wang, G. L. A comprehensive catalog of the lysine-acetylation targets in rice (Oryza sativa) based on proteomic analyses. *J. Proteomics* **2016**, *138*, 20−29.
(58) Yang, Y.; Tong, M.; Bai, X.; Liu, X.; Cai, X.; Luo, X.; Zhang, P.; Cai, W.; Vallée, I.; Zhou, Y.; Liu, M. Comprehensive proteomic analysis of lysine acetylation in the foodborne pathogen trichinella spiralis. *Front. Microbiol.* **2018**, *8*, 2674.
(59) Shao, J.; Xu, D.; Hu, L.; Kwan, Y. W.; Wang, Y.; Kong, X.; Ngai, S. M. Systematic analysis of human lysine acetylation proteins and accurate prediction of human lysine acetylation through bi-relative adapted binomial score Bayes feature representation. *Mol. BioSyst.* **2012**, *8*, 2964−2973.
(60) Zhou, X.; Qian, G.; Yi, X.; Li, X.; Liu, W. Systematic analysis of the lysine acetylome in Candida albicans. *J. Proteome Res.* **2016**, *15*, 2525−2536.
(61) Kachroo, A.; Kachroo, P. Fatty acid-derived signals in plant defense. *Annu. Rev. Phytopathol.* **2009**, *47*, 153−176.
(62) Gerhardt, B. Fatty acid degradation in plants. *Prog. Lipid Res.* **1992**, *31*, 417−446.
(63) Cooper, T. G.; Beevers, H. Beta oxidation in glyoxysomes from castor bean endosperm. *J. Biol. Chem.* **1969**, *244*, 3514−3520.
(64) Dym, O.; Eisenberg, D. Sequence-structure analysis of FAD-containing proteins. *Protein Sci.* **2001**, *10*, 1712−1728.
(65) Janssen, U.; Davis, E. M.; Le Beau, M. M.; Stoffel, W. Human mitochondrial enoyl-CoA hydratase gene (ECHS1): structural organization and assignment to chromosome 10q26.2-q26.3. *Genomics* **1997**, *40*, 470−5.
(66) Hillmer, P.; Gottschalk, G. Solubilization and partial characterization of particulate dehydrogenases from Clostridium kluyveri. *Biochim. Biophys. Acta Enzymol.* **1974**, *334*, 12−23.

https://doi.org/10.1021/acsomega.2c03917
ACS Omega 2022, 7, 32496−32511

(67) Fukao, T. Thiolases (Acetyl-CoA Acyltransferases). In *Wiley Encyclopedia of Molecular Medicine*; Burchell, J., Taylor-Papadimitriou, J., Eds.; John Wiley & Sons: New Jersey, 2002; pp 3125−3129.
(68) Zhang, D.; Yu, W.; Geisbrecht, B. V.; Gould, S. J.; Sprecher, H.; Schulz, H. Functional characterization of Δ3,Δ2-Enoyl-CoA isomerases from rat liver. *J. Biol. Chem.* **2002**, *277*, 9127−9132.
(69) Engeland, K.; Kindl, H. Purification and characterization of a plant peroxisomal delta 2, delta 3-enoyl-CoA isomerase acting on 3-cis-enoyl-CoA and 3-trans-enoyl-CoA. *Eur. J. Biochem.* **1991**, *196*, 699−705.
(70) Sonnewald, U. Glutamate synthesis has to be matched by its degradation - where do all the carbons go? *J. Neurochem.* **2014**, *131*, 399−406.
(71) Wu, X.; Oh, M. H.; Schwarz, E. M.; Larue, C. T.; Sivaguru, M.; Imai, B. S.; Yau, P. M.; Ort, D. R.; Huber, S. C. Lysine acetylation is a widespread protein modification for diverse proteins in arabidopsis. *Plant Physiol.* **2011**, *155*, 1769−1778.
(72) Salvato, F.; Havelund, J. F.; Chen, M.; Rao, R. S.; Rogowska-Wrzesinska, A.; Jensen, O. N.; Gang, D. R.; Thelen, J. J.; Møller, I. M. The potato tuber mitochondrial proteome. *Plant Physiol.* **2014**, *164*, 637−653.
(73) Li, S.; Lyu, S.; Liu, Y.; Luo, M.; Shi, S.; Deng, S. Cauliflower mosaic virus P6 Dysfunctions Histone Deacetylase HD2C to Promote Virus Infection. *Cells* **2021**, *10*, 2278.
(74) Zhang, B.; Zhang, L.; Li, F.; Zhang, D.; Liu, X.; Wang, H.; Xu, Z.; Chu, C.; Zhou, Y. Control of secondary cell wall patterning involves xylan deacetylation by a GDSL esterase. *Nat. Plants* **2017**, *3*, 17017.
(75) Lim, G. H.; Singhal, R.; Kachroo, A.; Kachroo, P. Fatty acid−and lipid-mediated signaling in plant defense. *Annu. Rev. Phytopathol.* **2017**, *55*, 505−536.
(76) Cury-boaventura, M. F.; Curi, R. Regulation of reactive oxygen species (ROS) production by C18 fatty acids in Jurkat and Raji cells. *Clin. Sci.* **2005**, *108*, 245−253.
(77) Zhu, F.; Xi, D. H.; Yuan, S.; Xu, F.; Zhang, D. W.; Lin, H. H. Salicylic acid and jasmonic acid are essential for systemic resistance against tobacco mosaic virus in Nicotiana benthamiana. *Mol. Plant-Microbe Interact.* **2014**, *27*, 567−577.
(78) Ryu, C. M.; Murphy, J. F.; Mysore, K. S.; Kloepper, J. W. Plant growth-promoting rhizobacteria systemically protect Arabidopsis thaliana against Cucumber mosaic virus by a salicylic acid and NPR1-independent and jasmonic acid-dependent signaling pathway. *Plant J.* **2004**, *39*, 381−392.
(79) Chu, J.; Xing, C.; Du, Y.; Duan, T.; Liu, S.; Zhang, P.; Cheng, C.; Henley, J.; Liu, X.; Qian, C.; Yin, B.; Wang, H. Y.; Wang, R.-F. Pharmacological inhibition of fatty acid synthesis blocks SARS-CoV-2 replication. *Nat. Metabol.* **2021**, *3*, 1466−1475.
(80) Min, Z.; Long, X.; Zhao, H.; Zhen, X.; Li, R.; Li, M.; Fan, Y.; Yu, Y.; Zhao, Y.; Qiao, J. Protein Lysine Acetylation in Ovarian Granulosa Cells Affects Metabolic Homeostasis and Clinical Presentations of Women With Polycystic Ovary Syndrome. *Front. Cell Dev. Biol.* **2020**, *8*, 567028.

https://doi.org/10.1021/acsomega.2c03917
ACS Omega 2022, 7, 32496−32511